

Photosensitized decomposition of *S*-nitrosothiols and 2-methyl-2-nitrosopropane

Possible use for site-directed nitric oxide production

Ravinder Jit Singh, Neil Hogg, Joy Joseph, B. Kalyanaraman*

Biophysics Research Institute, Medical College of Wisconsin 8701 Watertown Plank Rd., P.O. Box 26509, Milwaukee, WI 53226, USA

Received 17 December 1994; revised version received 10 January 1995

Abstract Irradiation of *S*-nitrosoglutathione (GSNO) with light ($\lambda = 550$ nm) resulted in the homolytic decomposition of GSNO to generate glutathionyl radical (GS \cdot) and nitric oxide (\cdot NO), which were monitored by ESR spectrometry. Inclusion of Rose Bengal (RB) resulted in a 9-fold increase in the quantum yield for \cdot NO production and also an increase in the rate of thiyl radical formation. The bimolecular rate constant for the interaction of triplet RB with GSNO has been estimated to be approximately 1.2×10^9 M $^{-1}$ s $^{-1}$ by competition with oxygen. Hematoporphyrin (HP) also enhanced the rate of \cdot NO production by 2–3-fold. 2-Methyl-2-nitrosopropane (MNP) decomposed on irradiation ($\lambda = 660$ nm) to form \cdot NO and *tert*-butyl radical. Aluminum phthalocyanine tetrasulphonate enhanced the rate of decomposition of MNP by 10-fold. These studies show that photosensitizers enhance the release of \cdot NO from donor compounds.

Key words: Nitric oxide; Thiyl radical; *S*-Nitrosoglutathione; 2-Methyl-2-nitrosopropane; Rose Bengal; Hematoporphyrin; Aluminum phthalocyanine tetrasulphonate

1. Introduction

Nitric oxide (\cdot NO) plays multiple roles in biological systems [1]. The precise biological effects of \cdot NO production depend largely upon the rate and localization of \cdot NO generation. Thus, \cdot NO can act both as a biological messenger and as a tumoricidal cytotoxin [2]. In endotoxic shock, for example, it has been shown to be advantageous to inhibit endogenous \cdot NO production while, paradoxically, administering an \cdot NO generating agent [3]. It is likely, therefore, that therapeutic strategies involving \cdot NO-donor compounds will require some specificity of both the rate and location of \cdot NO production. \cdot NO has been implicated in macrophage-mediated tumor cell killing through the inhibition of mitochondrial enzyme activity and DNA synthesis in target tumor cells [2]. \cdot NO donors such as *S*-nitrosothiols have been proposed as reservoirs of \cdot NO in vivo due to their higher stability in comparison with \cdot NO. These compounds exhibit a range of pharmacological properties [4–7]. The mode of action of these compounds is generally attributed to the activity of \cdot NO released on homolytic decomposition of the S-NO bond [8–10]. Recently, *S*-nitrosoglutathione (GSNO) has been shown to be significantly more toxic to HL-60 leukemia cells in the presence of light than in the dark [11].

Photodynamic sensitizers have been reported to produce active oxygen species by Type II and Type I mechanisms. Localized production of singlet oxygen (1O_2) and superoxide radicals

(O_2^-) as cytotoxic and antiviral agents has been achieved in photodynamic therapy (PDT) [12,13]. Since \cdot NO exhibits tumoricidal and antiviral activity [2,14], it may be possible to exploit photosensitized \cdot NO production in clinical PDT. In this study, we show that photosensitizers such as Rose Bengal (RB) and aluminum phthalocyanine tetrasulphonate (AlPcS) can increase \cdot NO production from *S*-nitrosothiols and C-nitroso compounds. Thus, localized \cdot NO release from photoactivation of such compounds may afford new therapeutic strategies in phototherapy.

2. Materials and methods

2.1. Chemicals

Rose Bengal (Aldrich Chemical Co., Milwaukee, WI), hematoporphyrin dihydrochloride (HP), 2-methyl-2-nitrosopropane dimer (Sigma Chemical Co., St. Louis, MO), aluminum phthalocyanine tetrasulphonate (AlPcS) (Porphyrin Products, Logan, UT) were used as supplied. *S*-nitrosoglutathione (GSNO) and *S*-nitroso-*N*-acetylpenicillamine (SNAP) were prepared as previously reported [15]. 2-(*p*-carboxyphenyl)-4,4,5,5-tetramethyl-imidazolin-3-oxide 1-oxyl (NNO) was used for monitoring the rate of \cdot NO production [16–18]. DMPO (Aldrich Chemical Co., Milwaukee, WI) was purified according to Kotake et al. [19].

2.2. ESR measurements

The samples were prepared in the dark on ice, taken into 50 μ l capillaries (Corning, NY), and sealed with Miniseal at each end. The capillary was placed in a quartz tube and irradiated with monochromatic light inside the ESR cavity.

ESR spectra were recorded on a Varian E109 spectrometer at 9.5 GHz employing 100 kHz field modulation. \cdot NO formation was measured by observing the decay of NNO. This compound has a characteristic five-line ESR spectrum that changes upon reaction with \cdot NO to a seven-line spectrum due to imino nitroxide (INO) formation. The decay of NNO is monitored by observing the decrease in signal intensity of the low field line of the NNO spectrum. Alternatively, the rate of INO production was monitored by observing the increase in signal intensity of the low-field line of the INO spectrum. The kinetics of DMPO/ \cdot SG adduct were followed by monitoring the low-field line of the spectrum. Aqueous solutions containing MNP with and without AlPcS were similarly irradiated inside the ESR cavity at room temperature.

2.3. Irradiation procedure and quantum yield measurements

Samples were irradiated with light from a Bausch and Lomb high-intensity monochromator, using an ILC PS300–1A xenon arc source (ILC Technology, Sunnyvale, CA). Prior to ESR measurements, photon fluence rates, at approximately 1 cm from the front of the cavity, were measured using a YSI Radiometer, Model 65A (Yellow Springs Instruments, Columbus, OH). The amount of light incident on the solution inside the ESR cavity was calculated by actinometry using hematoporphyrin and 2,2,6,6-tetramethyl-4-piperidine *N*-oxyl [20]. It was assumed that $I_a = I_0 (1 - 10^{-\epsilon cl})$, where I_a is the amount of light absorbed by *S*-nitrosothiol, I_0 is the amount of light incident on the sample, ϵ is the molar extinction coefficient, c is the concentration of *S*-nitrosothiol, and l is the path length.

*Corresponding author. Fax: (1) (414) 266 8515.

3. Results

3.1 Rose Bengal-sensitized decomposition of *S*-nitrosothiols

S-nitrosothiols possess absorption maxima in the range of $\lambda = 320\text{--}360\text{ nm}$ and $\lambda = 550\text{--}600\text{ nm}$ [8]. GSNO absorbs at 330 nm ($\epsilon_{\text{max}} = 767\text{ M}^{-1}\text{ cm}^{-1}$) and has very weak absorption in the visible region at $\lambda = 550\text{ nm}$ ($\epsilon_{\text{max}} = 13\text{ M}^{-1}\text{ cm}^{-1}$). Similarly, SNAP has absorption in the visible region at $\lambda = 590\text{ nm}$ ($\epsilon_{\text{max}} = 11\text{ M}^{-1}\text{ cm}^{-1}$). RB has an absorption band with $\lambda_{\text{max}} = 550\text{ nm}$, which overlaps considerably with the band of *S*-nitrosothiols in the visible region (Fig. 1). RB has been widely used as a photosensitizer due to its high triplet yield (0.7) and high molar absorption coefficient ($\epsilon_{\text{max}} = 1 \times 10^5\text{ M}^{-1}\text{ cm}^{-1}$ at $\lambda = 550\text{ nm}$) [21]. This makes energy transfer between triplet state of RB and the triplet of *S*-nitrosothiols plausible. This transfer of energy may sensitize the homolytic cleavage of the S–N bond of *S*-nitrosothiols and increase the rate of $\cdot\text{NO}$ production.

$\cdot\text{NO}$ production was not observed during incubation of GSNO (1 mM) and NNO (125 μM) in the dark. However, upon illumination with light ($\lambda = 550\text{ nm}$), the production of $\cdot\text{NO}$ was observed (Fig. 2). The initial rate of decay of NNO, due to reaction with $\cdot\text{NO}$ generated from photochemical decomposition of GSNO, was greatly enhanced in the presence of RB (100 μM) (Fig. 2). RB alone had no effect in the presence and absence of light indicating that neither RB nor $^1\text{O}_2$ react with NNO (data not shown). $\cdot\text{NO}$ production was more rapid when the reaction was conducted under nitrogen (Fig. 2). This probably represents competition of GSNO and oxygen for triplet state RB. Neither photobleaching nor cytochrome *c* reduction was observed during irradiation ($\lambda = 550\text{ nm}$) of RB (10 μM) in the presence of GSNO (100 μM). However, irradiation of RB and NADH (20 μM) resulted in superoxide-dependent reduction of cytochrome *c* and photobleaching (data not shown). RB also enhanced the rate of $\cdot\text{NO}$ production from SNAP and *S*-nitroso-*N*-acetylcysteine (SNAC) in the presence of light. The

quantum yield of GSNO decomposition increased from 0.026 ± 0.002 to 0.225 ± 0.01 upon irradiation with RB. Similarly, the quantum yields for SNAP decomposition increased from 0.039 ± 0.007 to 0.4 ± 0.01 and for SNAC from 0.128 ± 0.004 to 1.03 ± 0.12 . Erythrosin, a xanthine photosensitizer [21] absorbing in the visible region $\lambda_{\text{max}} = 526\text{ nm}$ with a triplet yield of 0.63, also enhanced the decomposition of GSNO to almost the same extent as RB (data not shown).

HP, a well studied photodynamic photosensitizer, has a Soret band at 390 nm with $\epsilon_{\text{max}} = 1.4 \times 10^5\text{ M}^{-1}\text{ cm}^{-1}$, but has relatively low molar extinction coefficient in the 500–600 nm region (Fig. 1). The triplet yield for HP has been reported to be 0.36 in aqueous medium [22]. HP in the dark or light ($\lambda = 550\text{ nm}$) had no effect on the ESR spectrum of NNO (data not shown). However, HP (100–350 μM) enhanced the rate of NNO decay by 2–3-fold in the presence of GSNO (1 mM) and light ($\lambda = 550\text{ nm}$) (Fig. 2). Under anaerobic conditions, the rate of NNO decay was further enhanced (data not shown).

Glutathionyl radical ($\text{GS}\cdot$) formed from photodecomposition of GSNO was trapped with 5,5-dimethyl-1-pyrroline-*N*-oxide (DMPO) to produce the characteristic ESR signal for the DMPO/ $\cdot\text{SG}$ adduct ($a_{\text{N}} = 14.9\text{ G}$; $a_{\text{H}} = 15.4\text{ G}$) (Fig. 3, inset) [23]. The DMPO/ $\cdot\text{SG}$ adduct increased in intensity to reach a maximum within 7 min. This maximum represents a steady-state level of DMPO/ $\cdot\text{SG}$ adduct concentration where the adduct is both forming and decaying at the same rate. The rate of DMPO/ $\cdot\text{SG}$ adduct formation increased by 5–6-fold in the presence of RB (100 μM) (Fig. 3). The bimolecular rate constant for the interaction between RB^* and GSNO has been determined from the slope of the plot of

$$1/\frac{d[\cdot\text{NO}]}{dt} \text{ vs. } 1/[\text{GSNO}]$$

(Fig. 4) according to the following equation:

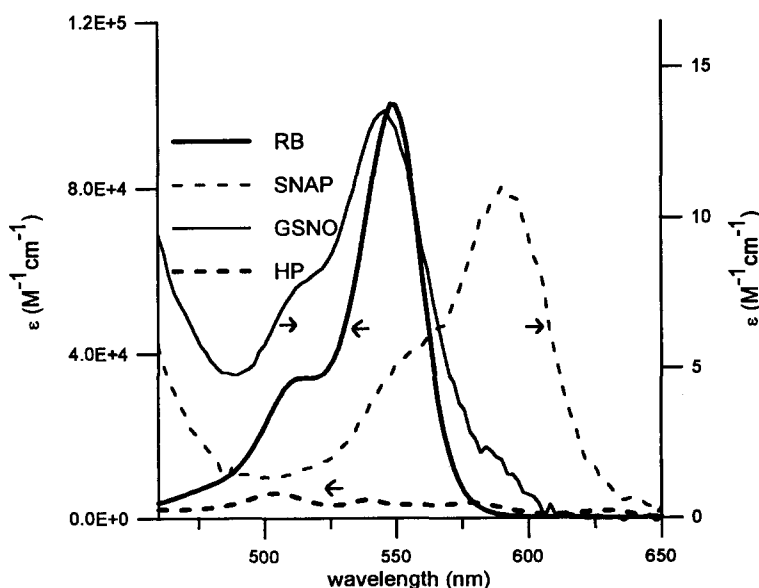


Fig. 1. Wavelength dependence of extinction coefficients for RB, HP, GSNO, and SNAP. The y-axis on the left is for RB and HP, and the y-axis on the right is for SNAP and GSNO as indicated by arrows.

$$\frac{d[\cdot\text{NO}]_{\text{max}}}{dt} = \frac{k_{\text{O}_2}[\text{O}_2]}{k_{\text{NO}}[\text{GSNO}]} + 1$$

where k_{O_2} and k_{NO} are the bimolecular rate constants between RB^* and O_2 or GSNO , respectively. This calculation assumes that oxygen competes for RB^* with GSNO . $d[\cdot\text{NO}]/dt$ is the initial rate of $\cdot\text{NO}$ formation for a particular concentration of GSNO , and

$$\frac{d[\cdot\text{NO}]_{\text{max}}}{dt}$$

is the maximum rate of $\cdot\text{NO}$ formation at a saturating concentration of GSNO . All rates of $\cdot\text{NO}$ formation were corrected for $\cdot\text{NO}$ release in the absence of RB . This analysis gives $k_{\text{NO}} = 1.2 \times 10^9 \text{ M}^{-1} \text{ s}^{-1}$ using a value of $1.6 \times 10^9 \text{ M}^{-1} \text{ s}^{-1}$ for k_{O_2} [24].

3.2. Aluminum phthalocyanine tetrasulphonate sensitized decomposition of 2-methyl 2-nitrosopropane

AIPcS was used to photosensitize the release of $\cdot\text{NO}$ from MNP. Specifically, AIPcS absorbs in the visible region at $\lambda = 660 \text{ nm}$ (Fig. 5) with a molar absorption coefficient of $2 \times 10^5 \text{ M}^{-1} \text{ cm}^{-1}$ and has triplet yield of 0.4 [25]. MNP in the monomeric form absorbs in the visible region at $\lambda = 660 \text{ nm}$ with a molar absorption coefficient of only $15 \text{ M}^{-1} \text{ cm}^{-1}$ [26]. The rate of $\cdot\text{NO}$ generation from MNP due to its photolytic decomposition with light of $\lambda = 660 \text{ nm}$ was monitored by following the decay of NNO in aqueous solution. A slow release of $\cdot\text{NO}$ from MNP was observed on irradiation; however, the rate of $\cdot\text{NO}$ formation increased markedly in the presence of AIPcS ($100 \mu\text{g}/\text{ml}$) (Fig. 6). A three-line ESR spectrum

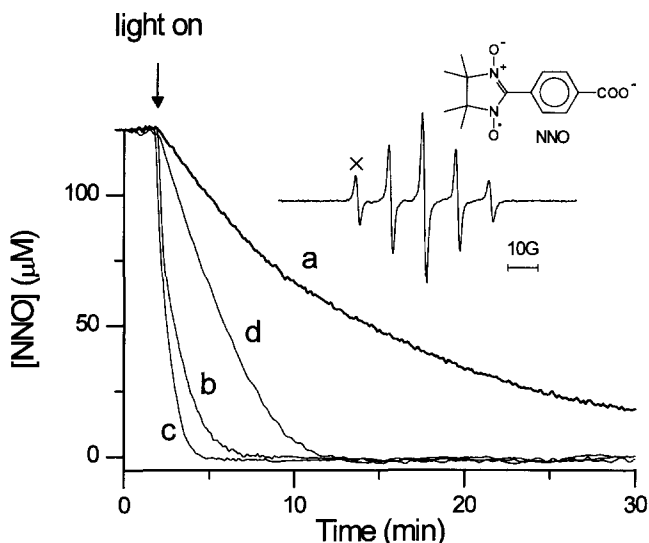


Fig. 2. $\cdot\text{NO}$ generation during photodecomposition of GSNO . Samples were prepared in the dark on ice, placed inside the ESR cavity and the decay of the low field line (marked 'x' in the inset spectrum) was monitored on irradiation (\downarrow with light ($\lambda = 550 \text{ nm}$, $I_0 = 85 \text{ watts}/\text{meter}^2$) at 20° C). (a) The decay of NNO ($125 \mu\text{M}$) in the presence of GSNO (1 mM) in air saturated PBS; (b) as (a) but in the presence of $100 \mu\text{M}$ RB ; (c) as (b) but under nitrogen; (d) as (a) but, in the presence of $250 \mu\text{M}$ HP . Spectrometer conditions: time constant, 1 s; scan time, 30 min; modulation amplitude, 1 G; microwave power, 1 mW.

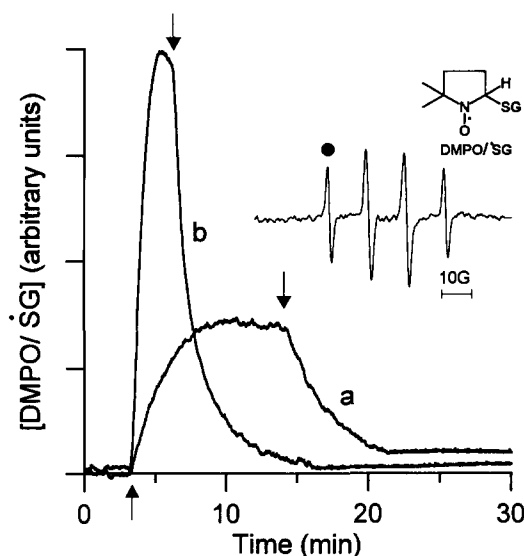


Fig. 3. DMPO/SG adduct formation and decay during photodecomposition of GSNO . The ESR spectrum of the DMPO/SG adduct was recorded after irradiation ($\lambda = 550 \text{ nm}$) of DMPO (20 mM) and GSNO (1 mM) in PBS (inset). The formation and decay of the adduct was monitored by following the change in the low-field line of the spectrum (marked '●' in the inset spectrum). (a) GSNO (1 mM) and DMPO (20 mM) in PBS during (f) and after (l) irradiation; (b) as (a), but in the presence of RB ($100 \mu\text{M}$). Spectrometer conditions: time constant, 1 s; scan time, 30 min; modulation amplitude, 5 G; microwave power, 20 mW.

($a_{\text{N}} = 17 \text{ G}$), corresponding to di-*tert*-butyl nitroxide, was obtained on photolysis ($\lambda = 630\text{--}660 \text{ nm}$) of MNP (20 mM) in PBS. The yield of di-*tert*-butyl nitroxide increased approximately 10-fold on irradiation of MNP (20 mM) in the presence of AIPcS ($100 \mu\text{g}/\text{ml}$) (data not shown).

4. Discussion

S-nitrosothiols have previously been reported to generate $\cdot\text{NO}$ on irradiation with light of 330 nm by reaction 1 [27–28].



S-nitrosothiols absorb in the visible region in the range of $\lambda = 550\text{--}600 \text{ nm}$ though the molar absorption coefficients are low. The excitation of GSNO with 550 nm radiation also leads to the formation of the same products as in Reaction (1), none of which absorbs light in this range. The excitation of GSNO in the presence of RB with $\lambda = 550 \text{ nm}$ radiation resulted in significant increase in the yields of $\text{GS}\cdot$ and $\cdot\text{NO}$. This implies that triplet RB , with a quantum yield of 0.75, transfers energy to the triplet state of *S*-nitrosothiols leading to efficient homolytic decomposition (Reactions (2) and (3))



It is possible to envisage electron transfer to RB^* from GSNO as occurs with reducing agents such as NADH and

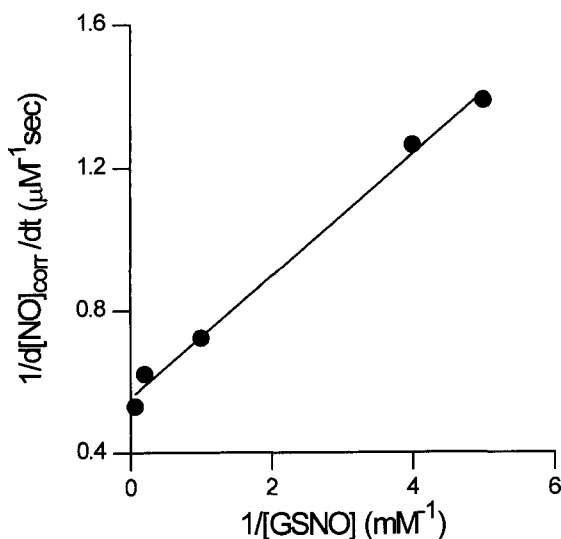


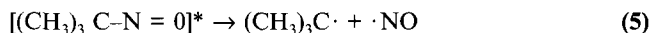
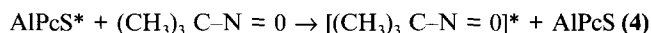
Fig. 4. Plot of $\frac{1/d[\cdot\text{NO}]_{\text{corr}}}{dt}$ vs. $1/[\text{GSNO}]$ for the determination of the rate constant between GSNO and RB^* . The rate of $\cdot\text{NO}$ production was calculated from the decay of the NNO spectrum during photoirradiation of 0.2, 0.25, 1, 5, and 15 mM GSNO in the presence of RB (100 μM).

GSH [29]. The result of this is the production of RB^* , which decays by either disproportionation, resulting in photobleaching of RB, or by reaction with oxygen generating superoxide. No photobleaching was observed during irradiation of RB with GSNO and the superoxide-dependent cytochrome *c* reduction was observed only during irradiation ($\lambda = 550$ nm) of RB (10 μM) and NADH (20 μM) and not during irradiation of RB (10 μM) and GSNO (100 μM). This suggests that electron-transfer from GSNO to RB^* is negligible. HP also enhanced the rate of GSNO decomposition by an energy transfer mechanism leading to a 2- to 3-fold enhanced rate of $\cdot\text{NO}$ production as shown by NNO decay studies.

Thiyl radicals can initiate oxidation/reduction reactions in biological systems. Thiyl radicals such as $\text{GS}\cdot$ can react with O_2 to form $\text{GSOO}\cdot$ or with GS^- to form the glutathione disulfide radical anion that can reduce O_2 to O_2^- [30]. The latter reaction is favored in an intracellular milieu because of the high intracellular concentration of glutathione. Thus, photosensitized decomposition of GSNO in cells can, in principle, result in the formation of $\cdot\text{NO}$ and O_2^- . The simultaneous production of O_2^- and $\cdot\text{NO}$ is clearly detrimental to cells due to formation of peroxynitrite, a potent oxidant [31].

The excitation of MNP with light of $\lambda = 660$ nm results in the formation of *tert*-butyl radical and $\cdot\text{NO}$ in very low yield. The *tert*-butyl radical is trapped by the parent compound MNP resulting in the formation of di-*tert*-butyl nitroxide radical [32]. The yield of di-*tert*-butyl nitroxide and $\cdot\text{NO}$ increased approximately 10 times when MNP was irradiated in the presence of AlPcS.

We propose Reactions (4–6) as the mechanism for photosensitized decomposition of MNP. Energy transfer from the triplet state of AlPcS to the triplet state of MNP leads to the enhanced homolytic decomposition to generate $\cdot\text{NO}$ and *tert*-butyl radical (Reaction 5). The *tert*-butyl radical is trapped by MNP to yield di-*tert*-butyl nitroxide (Reaction 6).



Previously, photosensitizers have been used to increase the yield and specificity of products formation as compared with *direct photochemical* reactions [33]. The mechanism for this effect has been reported to be energy transfer from the triplet state of the photosensitizer to the triplet state of an acceptor. Photosensitized decomposition of $\cdot\text{NO}$ donors as shown in the present study may provide a mechanism for localized release of $\cdot\text{NO}$ in high yield. It is known that during PDT, rapid tumor

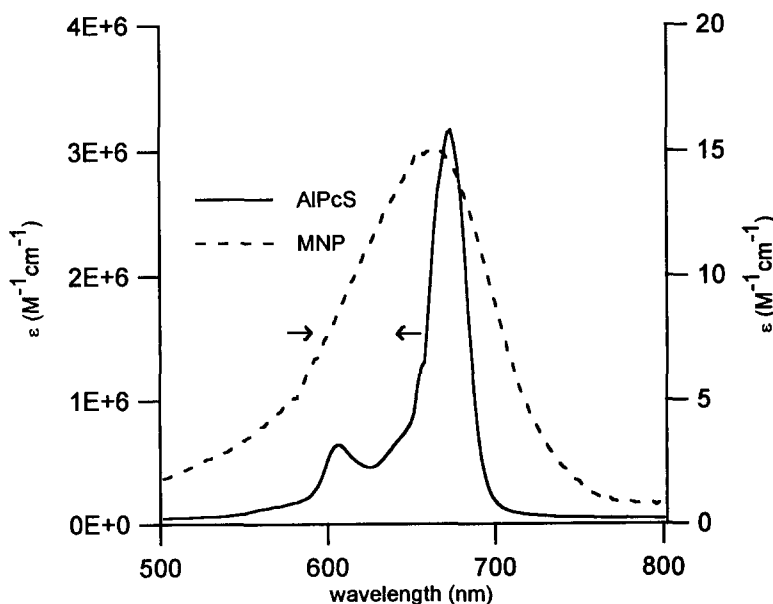


Fig. 5. Wavelength dependence of extinction coefficient for AlPcS and MNP. The y-axis on the left is for AlPcS and on the right is for MNP as indicated by arrows.

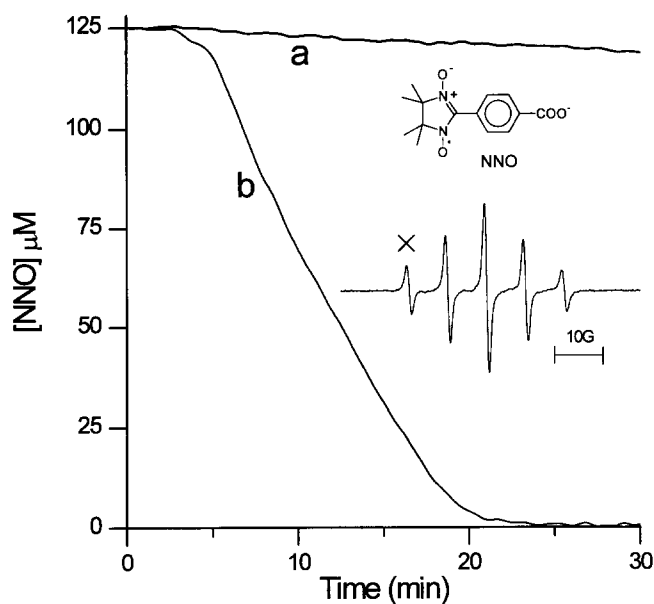


Fig. 6. $\cdot\text{NO}$ generation during photodecomposition of MNP ($\lambda = 660$ nm). (a) The decay of low-field line (marked 'x' the inset) NNO ($125 \mu\text{M}$) during the photodecomposition of MNP (20 mM) was monitored in air-saturated PBS on irradiation ($\lambda = 660$ nm); (b) as (a) but in the presence of $100 \mu\text{g/ml}$ AlPcS. Spectrometer conditions were as in Fig. 2.

hypoxia is achieved secondarily to microvascular stasis and thrombosis [34–35]. Furthermore, clinical PDT is apparently limited by the presence of preexisting hypoxic areas within the tumor. Therefore, these nitroso compounds might act as light-dependent hypoxic sensitizers by augmenting tumor-cell killing through generation of toxic levels of $\cdot\text{NO}$. The present modality may also be used to exploit the antimicrobial and antiviral activity of $\cdot\text{NO}$ in phototherapy [15].

In conclusion, we show that the photodecomposition of S-nitroso and C-nitroso compounds to generate $\cdot\text{NO}$ occurs by homolytic cleavage to form thiyl and carbon-centered radicals, respectively. $\cdot\text{NO}$ release can be dramatically enhanced in the presence of photodynamic sensitizers such as RB and AlPcS.

Acknowledgements: This research has been supported by NIH grants CA49089 and RR01008. We also thank Dr. James Thomas for thoughtful input.

References

[1] Moncada, S. (1992) *Acta Physiol. Scand.* 145, 201–227.
 [2] Stuehr, D.J., Gross, S.S., Sakuma, I., Levi, R. and Nathan, C.F. (1989) *J. Exp. Med.* 169, 1011–1020.
 [3] Nava, E., Palmer, R.M.J. and Moncada, S. (1992) *J. Cardiovasc. Pharmacol.* 20, S132–134.
 [4] Venturini, C.M., Palmer, R.M.J. and Moncada, S. (1993) *J. Pharmacol. Exp. Therapeut.* 266, 1497–1500.

[5] Mathews, W.R. and Kerr, S.W. (1993) *J. Pharmacol. Exp. Therapeut.* 267, 1529–1532.
 [6] Stamler, J.S. and Loscalzo, J. (1991) *J. Am. Coll. Cardiol.* 18, 1529–1536.
 [7] Stamler, J.S., Jaraki, O., Osborne, J., Simon, D.I., Keaney, J., Vita, J., Singel, D., Valeri, C.R. and Loscalzo, J. (1992) *Proc. Natl. Acad. Sci. USA* 89, 7674–7677.
 [8] Keaney Jr., J.F., Simon, D.I., Stamler, J.S., Jaraki, O., Scharfstein, J., Vita, J.A. and Loscalzo, J. (1993) *J. Clin. Invest.* 91, 1582.
 [9] Barrett, J., Fitzgibbons, T.J., Glauser, J., Still, R. H., Young, R.W. (1966) *Nature* 211, 848.
 [10] Stamler, J.S., Simon, D.I., Osborne, J.A., Mullins, M.E., Jaraki, O., Michel, T., Singel, D.J. and Loscalzo, J. (1992) *Proc. Natl. Acad. Sci. USA* 89, 444–448.
 [11] Sexton, D.J., Muruganandam, A., Mckenny, D.J. and Mutus, B. (1994) *Photochem. Photobiol.* 59, 463–467.
 [12] Henderson, B.W. and Dougherty, T.J. (1992) *Photochem. Photobiol.* 55, 145–157.
 [13] Seiber, F., Krueger, G.J., O'Brien, J.M., Schober, S.L., Sesenbrenner, L.L. and Sharkis, S.J. (1989) *Blood* 73, 345–300.
 [14] Karupiah, G., Xie, O., Buller, R.M.L., Nathan, C., Duarte, C. and MacMicking, J.D. (1993) *Science* 261, 1445–1448.
 [15] Field, L., Dilts, R.V., Ravichandran, R., Lenhert, P. G. and Carnahan, G.F. (1978) *J. Chem. Soc. Chem. Commun.* 249–250.
 [16] Akaike, T., Yoshida, M., Miyamoto, Y., Sato, K., Kohno, M., Sasamoto, K., Miyazaki, K., Ueda, S. and Maeda, H. (1993) *Biochemistry*, 32, 827–832.
 [17] Joseph, J., Kalyanaraman, B. and Hyde, J.S. (1993) *Biochem. Biophys. Res. Commun.* 192, 926–934.
 [18] Hogg, N., Singh, R.J., Joseph, J., Neese, F., Kalyanaraman, B. (1995) *Free Rad. Res. Commun.* (in press).
 [19] Kotake, Y., Reinke, L.A., Tanigawa, T. and Koshida, H. (1994) *Free Rad. Biol. Med.* 17, 215–223.
 [20] Moan, J., Hovik, B. and Wold, E. (1979) *Photochem. Photobiol.* 80, 623–624.
 [21] Neckers, D.C. (1989) *J. Photochem. Photobiol.* 47, 1–29.
 [22] Blum, A. and Grossweiner, L.I. (1985) *Photochem. Photobiol.* 41, 27–32.
 [23] Josephy, P.D., Rehorek, D. and Janzen, E.G. (1984) *Tetrahedron Lett.* 25, 1685–1688.
 [24] Lee, P.C.C. and Rodgers, M.A.J. (1987) *Photochem. Photobiol.* 45, 79–86.
 [25] Sonoda, M., Krishna, C.M. and Riesz, P. (1987) *Photochem. Photobiol.* 46, 625–631.
 [26] Calvert, J.G. and Pitts Jr., J.N. (1966) In: *Photochemistry*, John Wiley, 454.
 [27] Butler, A.R. and Williams, D.L.H. (1993) *Chem. Soc. Rev.* 22, 233.
 [28] McAninly, J., Williams, D.L.H., Askew, S.C., Butler, A.R. and Russell, C. (1993) *J. Chem. Soc. Chem. Commun.* 1758–1759.
 [29] Sarna, T., Zajac, J., Bowman, M.K. and Truscott, T.G. (1991) *J. Photochem. Photobiol. A: Chem.* 60, 295–310.
 [30] Winterbourn, C.C. (1993) *Free Rad. Biol. Med.* 14, 85–90.
 [31] Radi, R., Beckman, J.S., Bush, K.M. and Freeman, B.A. (1991) *Arch. Biochem. Biophys.* 288, 481–487.
 [32] Chamulitrat, W., Jordan, S.J., Mason, R.P., Saito, K. and Cutler, R.G. (1993) *J. Biol. Chem.* 268, 11520–11527.
 [33] Hammond, G.S., Salteil, J., Lamola, A.A., Turro, N.J., Bradshaw, J.S., Cowan, D.O., Counsell, R.C., Vogt, V. and Dalton, C. (1964) *J. Am. Chem. Soc.* 86, 3197–3217.
 [34] Chaudhuri, K., Keck, R.W. and Selman, S.H. (1987) *Photochem. Photobiol.* 46, 823–827.
 [35] Gillisen, M.J., Wit, L.E.A., Star, W.M., Koster, J. F. and Sluiter, W. (1993) *Cancer Res.* 53, 2548–2552.